

IRON ABUNDANCES IN HYDRODYNAMICAL SIMULATIONS OF GALAXY CLUSTERS

R. Valdarnini

SISSA, Via Beirut 2-4, 34014 Trieste, Italy



Hydrodynamical SPH simulations of galaxy clusters are used to investigate the metal enrichment of the intracluster medium. The final metallicity abundances of the simulated clusters are determined according to the numerical resolution and a number of model parameters. For a fiducial set of model prescriptions the results of the simulations indicate iron abundances in broad agreement with data. Final X-ray properties are not sensitive to the heating of the ICM. This supports a scenario where the ICM evolution of cool clusters is driven by radiative cooling.

1 Introduction

A large set of observations shows that the ICM of galaxy clusters is rich in metals (see ^{9,14} and references cited therein). Abundance gradients have also been measured ^{8,7,5}. For instance, Ezawa et al. ⁸ found a decrease in the iron abundance of AWM7 from $\simeq 0.5$ solar in the center to $\simeq 0.2$ solar at a distance of $\simeq 500Kpc$. These measurements provide strong support for the supernova (SN) scenario as heating source for the ICM.

The relative abundance of the heavy elements can then be used to constrain the enrichment mechanism of the ICM and the energy input from SNe. Analysis of the spatial distribution of metallicity gradients is also important for discriminating among the proposed enrichment scenarios ⁷. Analytical estimates of the energy input can be substantially different according to the assumed spatial distribution of the ICM metals and the efficiency of transferring the kinetic energy released in a SN explosion to the ambient gas ¹¹. Hydrodynamical simulations of galaxy clusters have the advantage over analytical methods that they take into account self-consistently the dynamical evolution of the gas. The implementation of a metal enrichment model for the ICM in hydrodynamical simulations is therefore important in order to investigate the ICM metal evolution. Chemical evolution in hydrodynamical simulations has already been considered in a variety of contexts ^{4,11,16,12,1}.

In this paper I present results from hydrodynamical SPH simulations of galaxy clusters, that have been used to investigate the dependence of the final iron abundance on a number of model parameters that control the ICM metal enrichment. This is done in order to obtain for the simulated clusters a final ICM distribution which can simultaneously fit a set of observational constraints, such as the observed iron abundances and the luminosity-temperature relation.

2 Simulations and results

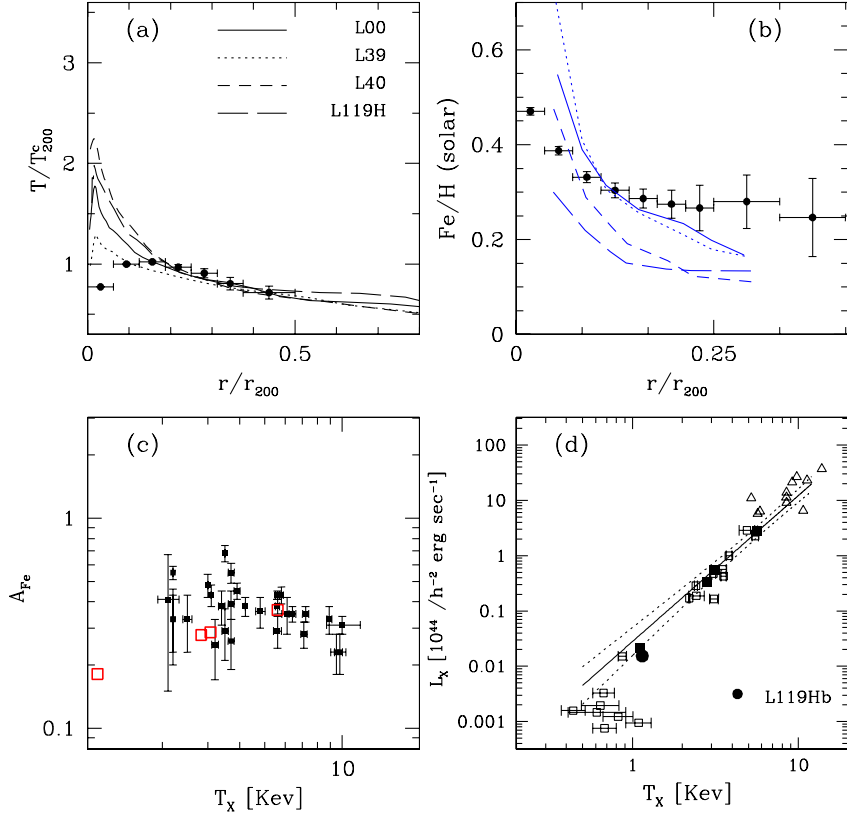
Hydrodynamical TREESPH simulations have been performed in physical coordinates for four test clusters. A detailed description of the procedure can be found in ¹⁹. The cosmological model is a flat CDM model, with vacuum energy density $\Omega_\Lambda = 0.7$, matter density parameter $\Omega_m = 0.3$ and Hubble constant $h = 0.7 = H_0/100 \text{Kms}^{-1} \text{Mpc}^{-1}$. $\Omega_b = 0.015h^{-2}$ is the value of the baryonic density. The four test clusters have decreasing virial mass and labels L00, L39, L40 and L119. The virial temperatures range from $\sim 6 \text{KeV}$ (L00) down to $\sim 1 \text{KeV}$ (L119). The simulations have a number of gas particles $N_g \simeq 22,600$. For L119 high resolution (H) runs have $N_g \simeq 70,000$. The cooling function of the gas particles depends also on the gas metallicity, and cold gas particles are subject to star formation. Once a star particle is created it will release energy into the surrounding gas through SN explosions of type II and Ia. The feedback energy (10^{51}erg) is returned to the nearest neighbor gas particles of the star particle, according to its lifetime and IMF ². SN explosions also inject enriched material into the ICM, thus increasing its metallicity with time. The adopted SNIa yields are those of Iwamoto et al. ¹⁰ (model W7). The yields of type II SN are those of Woosley & Weaver ²⁰ (model B). For each star particle the ejected masses of metals are calculated at each time step and distributed among the gas neighbors (~ 32) of the star particle. For the smoothing spline a common choice is the SPH kernel ^{16,12}. The profiles shown in the Figure are for a uniform deposition of metals.

The projected emission weighted temperature profiles are plotted as a function of the rescaled radius in panel (a). Data points are the mean error-weighted temperature profiles of 11 cooling flow clusters from De Grandi & Molendi ⁶. Each smoothed profile has been rescaled to match the last data point. There is a remarkable agreement of the simulated profiles with data, the only important exception being for the two innermost bins. The increase of the cluster temperature at the centre is a consequence of the entropy conservation during the galaxy formation and the subsequent removal of low-entropy gas ²¹. A possible explanation for this discrepancy with the data lies in the fact that the temperatures being measured are spectral temperatures ¹³.

The projected metallicity profiles are displayed as a function of distance in panel (b). The data points are the mean profile from the nine cooling flow clusters of De Grandi & Molendi ⁵. The iron profiles of L00 and L39 are the ones which are in better agreement with data. The overall shape of L40 is similar to that of the other two runs, but has a lower amplitude. The systematic difference between the profiles of runs L39 and L40 is mostly due to the different dynamical histories of the two clusters. Therefore, there are uncertainties in the final profiles which can be as high as $\sim 50\%$ and are related to the cluster dynamical evolution. At outer radii all of the profiles show a radial decay steeper than that of data points, which in fact can be considered to have an almost constant profile. It appears very difficult to modify the model parameters of the simulations in such a way that the simulated profiles match the data points at the outer radii, without also increasing central abundances.

The iron profile of L119H is inconsistent with the data points, the iron abundances being smaller at all radii. This is the coldest of the four test clusters ($T_X \sim 1 \text{KeV}$). The averaged observed profile is that of 9 cooling flow clusters, with minimum temperatures $\gtrsim 4 \text{KeV}$. Without measured profiles for cool clusters it is therefore difficult to put observational constraints on the different model parameters from the simulated profiles.

Global values $A_{Fe} = M_{Fe}/M_H$ of the iron abundances for the simulated clusters (open



squares) are compared in panel (c) with the estimated values (filled squares) for the nearby cluster sample of Matsumoto et al. ¹⁴. There is good agreement with data, but L119H has $A_{Fe} \simeq 0.2$, which is about a factor \sim two smaller than that expected from extrapolating the sample average below the minimum cluster sample temperature ($\simeq 2\text{KeV}$). For cool clusters there is the clear tendency in the simulations to produce a smaller amount of iron than that inferred from observations.

Finally, the values of the bolometric X-ray luminosity are shown in panel (d) as a function of the cluster temperature. Mass-weighted temperatures have been used as unbiased estimators of the spectral temperatures ¹³. Data points (open squares) are those of Fig. 11 of Tozzi & Norman ¹⁸. For the sake of clarity, not all of the points of their Figure are plotted in the panel. For a consistent comparison with data, a central region of size $50h^{-1}\text{Kpc}$ has been excised ¹⁵, in order to remove the contribution to L_X of the central cooling flow. The continuous line is the best-fit ¹⁵ $L_X = 3.11 \cdot 10^{44} h^{-2} (T/6\text{KeV})^{2.64}$. The dashed lines are the 68% confidence intervals. The L_X of the simulations are in excellent agreement with the data over the entire range of temperatures. An additional run (L119Hb) has been performed for the cluster with the lowest temperature, the only difference with respect to L119H being a SN feedback energy of 10^{50} erg for both SNII and Ia. As can be seen, the final L_X of the run L119Hb is very similar to that of L119H. This demonstrates that final X-ray luminosities of the simulations are not sensitive to the amount of SN feedback energy that has heated the ICM. In fact, a simulation run with zero SN energy being returned to the ICM yields very similar results. These findings are particularly relevant in connection with the recent proposal ³ that the X-ray properties of the ICM are driven by the efficiency of galaxy formation, rather than by heating due to non-gravitational processes. To summarize, the metal enrichment of the ICM can be modeled in

hydrodynamical SPH simulations with a number of model parameters. The results show final iron abundance gradients in broad agreement with the data. Moreover, the final X-ray properties of the simulated clusters are not sensitive to the amount of SN energy that has heated the ICM. These findings support a scenario where the ICM evolution of cool clusters is dominated by cooling and galaxy formation.

References

1. Aguirre, A. *et al.*, ApJ **561**, 521 (2001)
2. Arimoto, N. & Yoshii, Y. A&A **173**, 23 (1987)
3. Bryan, G. L. ApJ **544**, L1 (2000)
4. Carraro G., Lia C. & Chiosi C. MNRAS **297**, 1021 (1998)
5. De Grandi, S. & Molendi, S. ApJ **551**, 153 (2001)
6. De Grandi, S. & Molendi, S. ApJ **567**, 163 (2002)
7. Dupke, R. A. & White R. ApJ **537**, 123 (2000)
8. Ezawa, H. *et al.*, ApJL **490**, 33 (1997)
9. Fukazawa, Y. *et al.*, MNRAS **313**, 21 (2000)
10. Iwamoto, K. *et al.*, ApJS **125**, 439 (1999)
11. Kravtsov, A. V. & Yepes, G. MNRAS **318**, 227 (2000)
12. Lia, C., Portinari, L. & Carraro, G. MNRAS **330**, 821 (2002)
13. Mathiesen, B. & Evrard, A. E. ApJ **546**, 100 (2001)
14. Matsumoto, H. *et al.*, PASJ **52**, 153 (2000)
15. Markevitch, M. ApJ **504**, 27 (1998)
16. Mosconi, M. B. *et al.*, MNRAS **325**, 34 (2001)
17. Navarro, J. & White, S.D.M. MNRAS **265**, 271 (1993)
18. Tozzi, P. & Norman, C. ApJ **546**, 63 (2001)
19. Valdarnini, R. ApJ **567**, 741 (2002)
20. Woosley, S. E. & Weaver, T. A. ApJS **101**, 181 (1995)
21. Wu, X.-P. & Xue, Y.-J. ApJ **569**, 112 (2002)